



Clusters of galaxies in the COSMOS field

Alexis Finoguenov¹ and the COSMOS team²

¹ Max-Planck-Institut für Extraterrestrische Physik, Giessenbachstraße, 85748 Garching, Germany

² <http://www.astro.caltech.edu/cosmos>

Abstract. We present the results of a search for galaxy clusters in the first 36 XMM-Newton pointings on the COSMOS field. We reach a depth for a total cluster flux in the 0.5–2 keV band of 3×10^{-15} ergs cm⁻² s⁻¹, having one of the widest XMM-Newton contiguous raster surveys, covering an area of 2.1 square degrees. Cluster candidates are identified through a wavelet detection of extended X-ray emission. Verification of the cluster candidates is done based on a galaxy concentration analysis in redshift slices of thickness of 0.1–0.2 in redshift, using the multi-band photometric catalog of the COSMOS field and restricting the search to $z < 1.3$ and $i_{AB} < 25$. We identify 72 clusters and derive their properties based on the X-ray cluster scaling relations. A statistical description of the survey in terms of the cumulative $\log(N > S) - \log(S)$ distribution compares well with previous results, although yielding a somewhat higher number of clusters at similar fluxes. The X-ray luminosity function of COSMOS clusters matches well the results of nearby surveys, providing a comparably tight constraint on the faint end slope of $\alpha = 1.93 \pm 0.04$. For the probed luminosity range of $8 \times 10^{42} - 2 \times 10^{44}$ ergs s⁻¹, our survey is in agreement with and adds significantly to the existing data on the cluster luminosity function at high redshifts and implies no substantial evolution at these luminosities to $z = 1.3$.

1. Introduction

Clusters of galaxies represent a formidable tool for cosmology (e.g. Borgani & Guzzo 2001; Rosati et al. 2002). As the largest gravitationally relaxed structures in the Universe, their properties are highly sensitive to the physics of cosmic structure formation and to the value of fundamental cosmological parameters, specifically the normalization of the power spectrum σ_8 and the density parameter Ω_M . Clusters are in principle “simple” systems, where the observed properties of the (diffuse) baryonic component should be easier to connect to the mass of the dark matter halo, compared to the complexity of the various processes (e.g. star formation and evolution, stellar and AGN feedback) needed to understand the galaxy formation. In particular in the X-ray band, where clusters can be defined and recognized as single objects, observable quantities like X-ray luminosity L_X and temperature T_X show fairly tight relations with the cluster mass (e.g. Reiprich & Böhringer 2002). Understanding these scaling relations apparently requires more ingredients than simple heating by adiabatic compression during the growth of fluctuations (Ponman et al. 2003). However, their very existence and relative tightness provides us with a way to measure the mass function (e.g. Pierpaoli et al. 2003) and power spectrum (Schuecker et al. 2003), via respectively the observed X-ray temperature/luminosity functions and the clustering of clusters, thus probing directly the cosmological model.

2. XMM-COSMOS

The 1.4 Msec XMM-Newton observations of the COSMOS field (Hasinger et al. 2007) provide coverage of an area of

2.1 square degree to unprecedented depth of 10^{-15} ergs cm⁻² s⁻¹. In this contribution we outline the major results of the survey, while technical details are presented in Finoguenov et al. (2007).

In Fig. 1 we overlay the X-ray contours corresponding to extended X-ray emission over the color-coded image of the structures identified via the photo-z galaxy selection. The brightness of the color is proportional to the number density of galaxies, while the color represents the average redshift.

2.1. Sample characteristics

Figure. 2 shows the $\log(N > S) - \log(S)$ relation of the COSMOS field clusters. Although with a somewhat higher normalization, the COSMOS $\log(N > S) - \log(S)$ is statistically consistent with RDCS results of Rosati et al. (2002) for the fluxes $S > 10^{-14}$ ergs cm⁻² s⁻¹. While a similarly higher normalization of the $\log N - \log S$ has also been reported for the XMM-LSS survey (Pierre et al. 2005) as well as for the 160 square degrees survey (Vikhlinin et al. 1998), an important difference between those surveys and the RDCS consists in extrapolation of the cluster flux beyond the detection radius. As no extrapolation has been done for RDCS, the difference in the results is due to higher flux being assigned to each source, and not due to the higher source density. At fluxes below 10^{-14} ergs cm⁻² s⁻¹ the XMM-COSMOS is the first survey to yield rich observational data, allowing us to determine the $\log(N > S) - \log(S)$ with good statistics down to $S \sim 10^{-15}$ ergs cm⁻² s⁻¹. We note that the prediction for no evolution in the luminosity function obtained by local

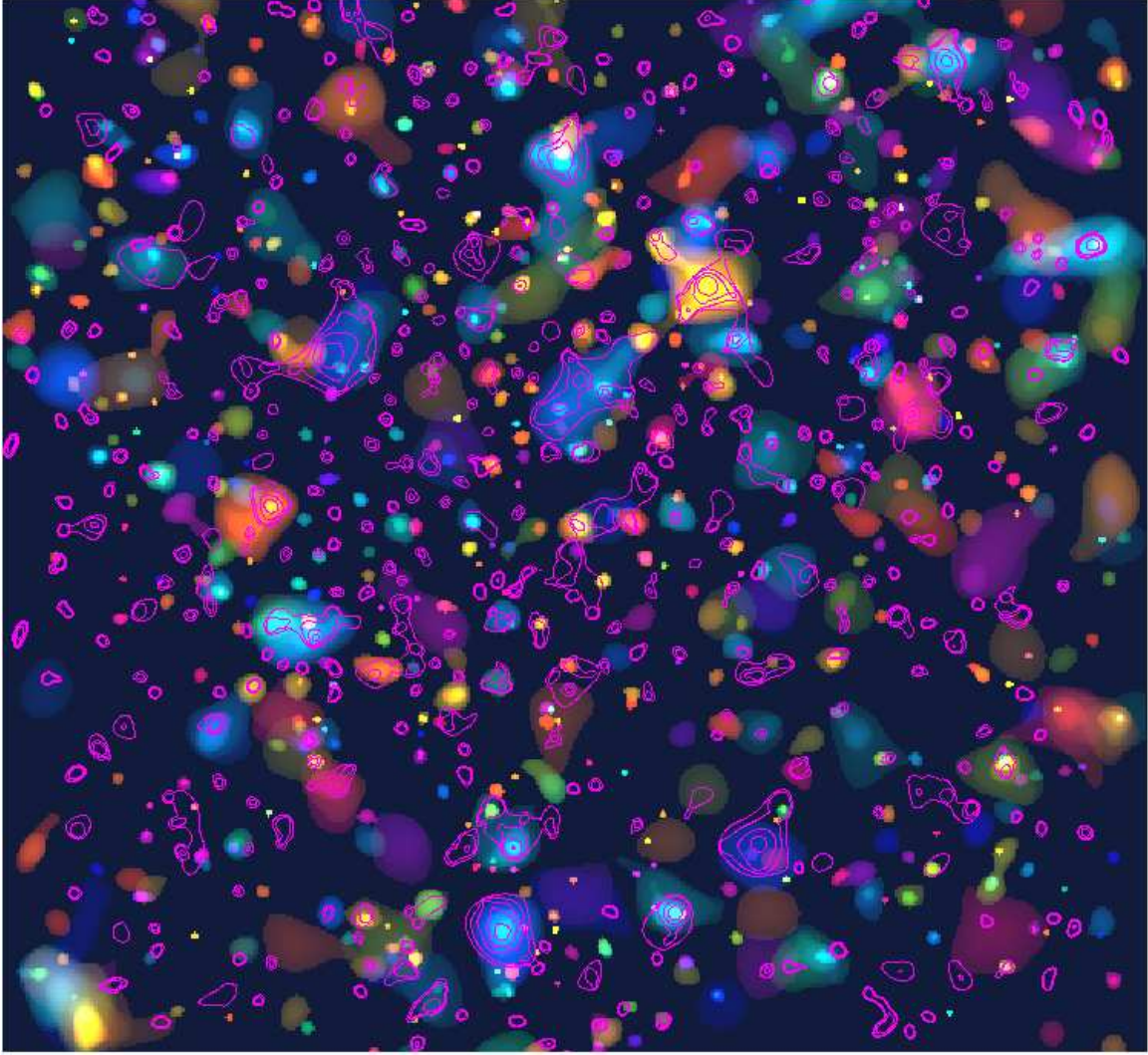


Fig. 1. The colors of COSMOS. The wavelet reconstruction of the early-type galaxy concentrations searched in the photo-z catalog is color-coded according to the average redshift: blue – 0.2, cyan – 0.4, green – 0.6, yellow – 0.8, red – 1.0. The magenta contours outline the diffuse X-ray emission, with some remaining contamination from the point sources. The image is 1.5 degrees on a side. The pixel size is $10''$ on a side.

surveys, as summarized in Rosati et al. (2002), provides a good fit to our cluster counts.

In Fig. 3 we plot the observed characteristics of the XMM-COSMOS cluster sample together with detection limits implied by both survey depth and our approach to search for clusters of galaxies. The solid gray line shows which sources cannot be detected as extended by our technique. The dotted grey line shows for which clusters the cores could be resolved in our method. The black lines show the detection limits of the survey achieved over 90, 50 and 10% of the total area. This comparison shows that with a given method it is possible to go a factor of 10 deeper without losing X-ray groups of galaxies that would appear point-like, which explains the success of the application of our cluster detection method to deep fields. Likewise, the clusters much larger than the detection cell, which are the brightest at each redshift, are all detected de facto. In a much shallower survey, where the detection limits would be similar to the short-dashed curve at

which the core of the cluster is larger than the selected detection cell, a problem with a fixed detection size might occur. Thus we conclude, that the success of the method is a result of a good match between the detection cell, the depth of the survey and the properties of X-ray emission of clusters of galaxies.

3. X-ray luminosity function

In the no-evolution case and in the absence of strong clustering, one expects to detect the clusters uniformly throughout the probed volume ($\langle V/V_{max} \rangle = 0.5$, Schmidt 1969). So, if any issues of incomplete identification, e.g. resulting from the use of the photo-z catalog, are important at some redshift (e.g. at very low redshifts or at very high redshifts), this would introduce a distortion in the distribution of clusters over the volume. To check if there are biases for some class of objects (e.g. low-luminosity objects), we plot in Fig. 4 the ratio between the volume towards the

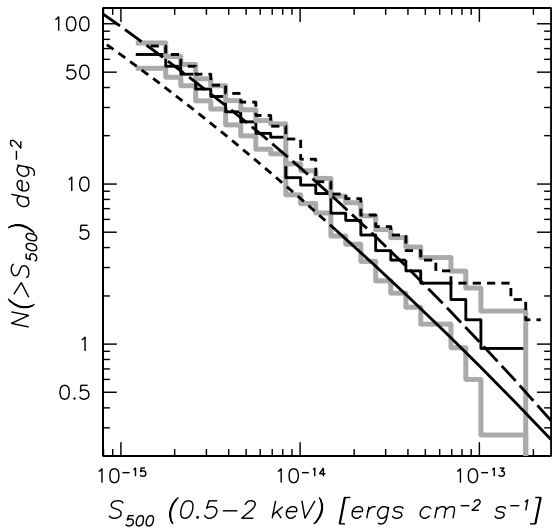


Fig. 2. Cumulative cluster number counts ($\log(N > S) - \log(S)$) for the COSMOS field. The solid histogram shows the data and grey histograms denote the 68% confidence interval. The black solid/short-dashed curve shows the results of the modeling of RDCS (Rosati et al. 2002), with the solid part corresponding to fluxes sampled by their data, while the short dashed line denotes the model prediction. The long dashed curve shows the prediction for no evolution in the luminosity function in Rosati et al. (2002), which provides a good fit to our data. The dashed histogram shows a typical difference due to assumption of the scaling relations.

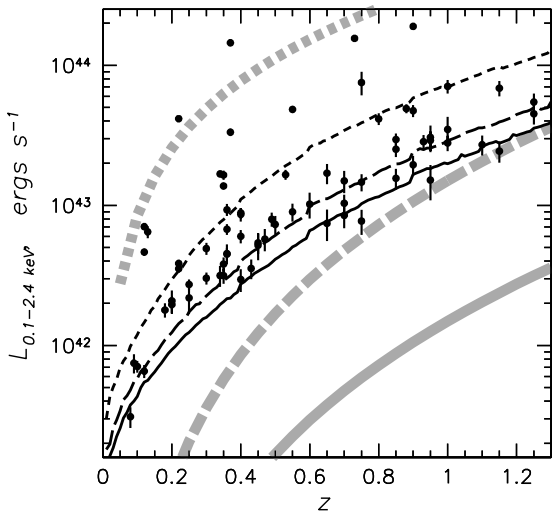


Fig. 3. Illustration of the cluster luminosity probed as a function of cluster redshift in the XMM COSMOS survey. Filled circles represent the detected clusters with error bars based on the statistical errors in the flux measurements only. Short-dashed, long-dashed and solid black lines show the flux detection limits associated with 90, 50 and 10% of the total area, respectively. Grey lines indicate the limits imposed by the detection method (i.e. due to the angular resolution of the XMM-Newton telescopes). Systems below the short-dashed grey line have unresolved cores, systems below the long-dashed grey line (none in our sample) suffer from oversubtraction of core emission. No system below the solid grey line can be detected as an extended source using the method described in this paper.

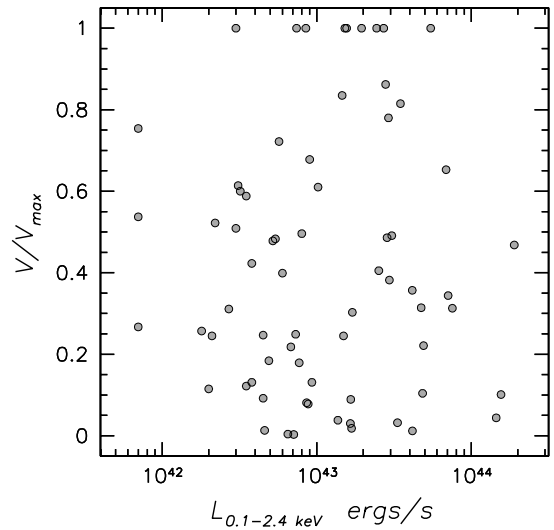


Fig. 4. Test for the sample redshift completeness (V/V_{\max}). The estimates exceeding 1 (due to the scatter in the flux-area relation) are substituted with 1. The number of clusters above and below 0.5 is roughly equal at all luminosities, indicating no large selection effects.

system and the maximum volume at which it could be detected. As some values exceed unity due to the scatter in the flux-area relation, we replaced them by unity for illustrative purposes. The numbers of clusters above and below 0.5 are roughly equal at all luminosities, indicating no large selection effects. The mean value of V/V_{\max} for the survey is equal to 0.48 ± 0.06 , which is consistent with 0.5 within the statistical errors. This is an important result in itself, that may illustrate that morphological changes observed in high-redshift clusters (Postman et al. 2005) do not cause strong redshift-dependent selection effects. It is clear, however, that any effects of incompleteness occurring at the 10% level would be hard to detect with the size of our sample.

Finally, in Fig. 5 we present the luminosity function of XMM COSMOS clusters. A comparison with the results of the REFLEX (Boehringer et al. 2001) and the BCS survey (Ebeling et al. 1997) displayed in Fig. 5 shows that, at the luminosity range probed by the COSMOS survey, the evolution in the luminosity function is not statistically significant.

The COSMOS data allow us to put tight constraints on the slope of the faint end of the luminosity function. To characterize it, we fitted a Schechter function to the data adopting the L_X^* and ϕ^* parameters in correspondence to the best fit values of BCS survey ($9.1 \times 10^{44} h_{50}^{-2}$ ergs/s $^{-1}$ and $7.74 \times 10^{-8} h_{50}^3$ Mpc $^{-3}$). We achieve an acceptable value of the reduced $\chi^2 = 0.7$ for 7 degrees of freedom and constrain the value of the slope to $\alpha = 1.93 \pm 0.04$ (where $dn/dL \propto L^{-\alpha}$), using the Gehrels (1986) approximations in calculating the confidence limits for the case of small number statistics. The value of the slope compares well with the BCS result of $\alpha = 1.85 \pm 0.09$. Our slope value is also within the uncertainty reported for the 160 square

degrees survey (Mullis et al. 2004). However, their use of the 0.5 – 2 keV energy band results in a somewhat lower value of the slope, and a strict comparison of luminosity functions is difficult. The lower number of groups in the REFLEX survey (dotted line in Fig. 5) is thought to be due to a combination of the small survey depth at low luminosities and a presence of a local southern void, where most of the survey area is located and whose effect has been demonstrated through differences within the sample (Böhringer et al. 2002).

To illustrate the lack of redshift evolution in the luminosity function, in Fig. 5 we split the sample in two redshift bins, 0–0.6 (dotted crosses) and 0.6–1.3 (solid crosses), retaining only the luminosity bins derived using at least three clusters. The two subsamples overlap only in a single luminosity bin, where the corresponding cluster abundances agree within the errors. Since the high-luminosities are well probed only at redshifts higher than 0.6, the good match between our measurements and the local luminosity function is an indication of the absence of a significant redshift evolution. This finding is in agreement with the results of Mullis et al. (2004), where detectable evolutionary effects are seen just above $L_x \sim 10^{44}$ ergs/s. We note that our measurements are of comparable quality to the existing data compiled in Mullis et al. (2004) and provide a refinement to the knowledge on the luminosity function at high redshifts. Finally, we note that both our cluster counts and the luminosity function are consistent with no evolution in the luminosity function in the $8 \times 10^{42} - 2 \times 10^{44}$ ergs s⁻¹ range. This provides further evidence in favor of a consistent modeling of the XMM-COSMOS survey sensitivity presented in this paper.

4. Summary

We present a description of our X-ray based cluster detection method and the first results of the cluster search using the XMM-COSMOS survey. Our flux range is $3 \times 10^{-15} - 10^{-13}$ erg cm⁻² s⁻¹ in the 0.5–2 keV band. We run a separate analysis of the photo-z catalog to identify 420 early-type galaxy concentrations, which provide an identification to 72 X-ray cluster candidates. We further present the statistics for those clusters in terms of $\log N - \log S$, dN/dz and dn/dL . By comparison with local cluster surveys, we find no evolution in cluster number abundance out to a redshift of 1.3 in the luminosity range of $L_{0.1-2.4\text{keV}} : 8 \times 10^{42} - 2 \times 10^{44}$ ergs s⁻¹. This further implies that the surface density of clusters detected in the flux range $10^{-15} - 10^{-14}$ erg cm⁻² s⁻¹ should correspond to the prediction of no evolution, higher than implied by Rosati et al. (2002). Such high surface density of clusters has been found by both COSMOS and XMM-LSS surveys (Pierre et al. 2005).

Acknowledgements. In Germany, the XMM-Newton project is supported by the Bundesministerium für Wirtschaft und Technologie/Deutsches Zentrum für Luft- und Raumfahrt (BMWI/DLR, FKZ 50 OX 0001), the Max-Planck Society and

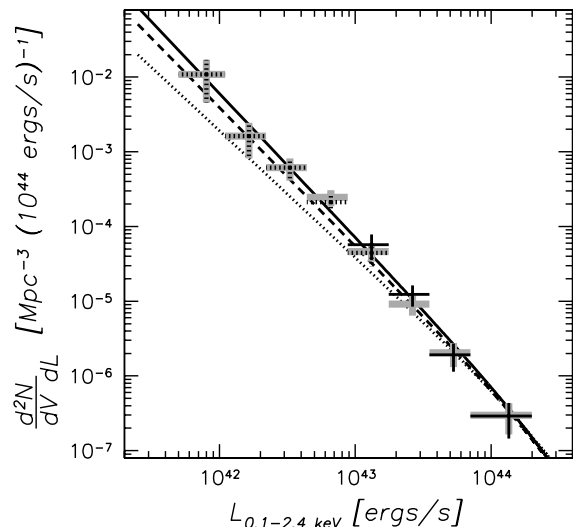


Fig. 5. Luminosity function of clusters in the COSMOS field. Dotted crosses indicate the data in the redshift range 0–0.6, grey points are the data in the redshift range 0–1.3 and solid crosses indicate the data in the redshift range 0.6–1.3. The dotted line shows the luminosity function of the REFLEX survey ($0 < z < 0.3$, Böhringer et al. 2001) and the dashed line shows the results of BCS survey (Ebeling et al. 1997), which illustrates the current uncertainty on the shape of the luminosity function at $z < 0.3$. The solid line shows the best fit to the COSMOS data.

the Heidenhain-Stiftung. Part of this work was supported by the Deutsches Zentrum für Luft- und Raumfahrt, DLR project numbers 50 OR 0207 and 50 OR 0405. We gratefully acknowledge the contributions of the entire COSMOS collaboration consisting of more than 70 scientists. AF acknowledges support from BMBF/DLR under grant 50 OR 0207.

References

- Böhringer, H., et al., 2001, A&A, 369, 826
- Böhringer, H., et al., 2002 ApJ, 566, 93
- Borgani, S. & Guzzo, L., 2001, Nature 409, 39
- Ebeling, H., et al., 1997, ApJ, 479, L101
- Finoguenov, A., et al., 2007, ApJS, COSMOS Special Issue
- Gehrels, N., 1986, ApJ, 303, 336
- Hasinger, G., et al., 2007, ApJS, COSMOS Special Issue
- Mullis, C. R., et al., 2004, ApJ, 607, 175
- Pierpaoli, E., et al., 2003, MNRAS, 342, 16
- Pierre, M., Pacaud, F., & XMM-LSS consortium, 2005, (astro-ph/0511184)
- Ponman, T. J., Sanderson, A. J. R., & Finoguenov, A., 2003, MNRAS, 343, 331
- Postman, M., et al., 2005, ApJ, 623, 721
- Reiprich, T. H. & Böhringer, H., 2002, ApJ, 567, 716
- Rosati, P., Borgani, S., & Norman, C., 2002, ARA&A, 40, 539
- Schmidt, M., 1969, ApJ, 151, 393
- Schuecker, P., et al., 2003, A&A, 398, 867
- Vikhlinin, A., et al., 1998, ApJ, 502, 558